Rovibrational cooling of photoassociated $^{85}Rb_2$ molecules at millikelvin temperature

Meng Wang, Bing-Kuan Lyu, Jing-Lun Li, Gao-Ren Wang, Mao-Du Chen, and Shu-Lin Cong*
School of Physics, Dalian University of Technology, Dalian 116024, China

(Received 19 January 2019; published 30 May 2019)

We investigate theoretically the rovibrational cooling of the $^{85}Rb_2$ molecule resulting from the photoassociation of $^{85}Rb_2$ atoms at millikelvin temperature. At several millikelvin temperature, the populations of the initial state and the photoassociated $^{85}Rb_2$ molecule are distributed on hundreds of rovibrational levels. In the laser rovibrational cooling process, the population of the photoassociated molecule is first transferred to the deep vibrational state $|\psi_{v''=39}\rangle$ and then further to the rovibrational ground state $|\psi_{v''=0,l=0}\rangle$ via the intermediate state $|\psi_{v'=42,l_e=1}\rangle$. After the cooling process is over, the population transferred from the intermediate state $|\psi_{v'=42,l_e=1}\rangle$ is fully distributed in the vibrational ground state $|v''=0\rangle$. Of the population in the vibrational ground state, 51.59% is concentrated in the rotational ground state $|l=0\rangle$, and the rest of population is distributed in the low rotational states $|l=1-3\rangle$.

DOI: 10.1103/PhysRevA.99.053428

I. INTRODUCTION

Cold and ultracold atoms and molecules possess some special properties and hence are widely applied to quantum information processing [1–3], fundamental physical constants measurement [4,5], ultracold chemistry [6], and so on. Photoassociation (PA) is an efficient way of preparing cold or ultracold molecules. In a photoassociation process, two atoms are associated into a molecule under the action of a laser field [7–15].

The molecule associated by a laser field usually lies in a large range of rovibrational levels of the excited electronic state [16–18]. In order to improve the efficiency of association, researchers often use a short or ultrashort shaped laser pulse to manipulate the photoassociation process, such as the chirped pulses and the slowly turned on and rapidly turned off laser pulses [19–22]. Because of the large bandwidth of an ultrashort pulse, a lot of vibrational and rotational levels are activated and populated in the photoassociation process [23]. Even if a continuous-wave laser with a very small bandwidth is applied, it can still excite a few rotational levels [24].

Temperature is one of the determinant factors in a photoassociation process. In the case of ultralow temperature, atomic scattering results mainly from the *s*-wave scattering [25]. With increasing temperature, high rotational and vibrational degrees of freedom are activated. The rotational barrier plays an important role in atomic collisions. A quasibound diatomic state trapped behind a rotational barrier can cause elastic scattering resonance, which is known as shape resonance [26–29]. The photoassociation probability can be enhanced by shape resonance in the scattering of ground-state atoms, because the shape resonance increases the amplitude of the wave function inside the centrifugal barrier [30]. The rotational barrier and the weight distribution of the initial state will be changed to some extent, which affects the photoassociation probability. The collisional energy at which the shape resonance occurs usually exceeds several hundred microkelvin or several millikelvin or even higher. For example, for the ^{85}Rb collisional atoms, the collisional energies in shape resonances for $l=$ 10, 14, and 18 are 10.1, 13.0, and 10.9 mK, respectively [31]. At higher temperature, the atomic scattering state can easily penetrate the rotational barrier due to the higher collisional energy. The association process mostly takes place at a short interatomic separation, which is in favor of the population increase of the photoassociated molecule on the deeply bound rovibrational levels of the excited electronic state [32]. Due to the thermodynamics effect, the Boltzmann weights will govern the population distribution on the rovibrational levels of the initial state [31]. At several millikelvin temperature, several hundred rovibrational levels of the initial state may be populated. Therefore, the existence of a thermodynamics effect will enlarge the population distribution range of rovibrational levels in the excited electronic state. Experimentally, the investigation of photoassociation at millikelvin or higher temperatures is feasible. Some important works have been performed. Gardner *et al*. investigated the collisions of doubly spin-polarized ^{85}Rb atoms and the photoassociation spectroscopy at millikelvin temperatures [33]. Zinner *et al*. studied the rovibrational spectra of Ca_2 molecules resulting from the photoassociation of Ca atoms at 3 mK [34]. Rybak and Levin *et al*. investigated experimentally the femtosecond photoassociation of hot Mg atoms at 1000 K [35,36].

For the purpose of application, the photoassociated molecules on the high vibrational and rotational levels of the excited electronic state need to be cooled to the rovibrational ground state or the deep rovibrational state of the ground electronic state. The rovibrational cooling of photoassociated molecules at ultralow temperature has been experimentally implemented. Aikawa *et al*. researched experimentally how to convert the laser-cooled atoms into ultracold molecules in the rovibrational ground state via photoassociation followed by stimulated Raman adiabatic passage (STIRAP) [37].

*shlcong@dlut.edu.cn

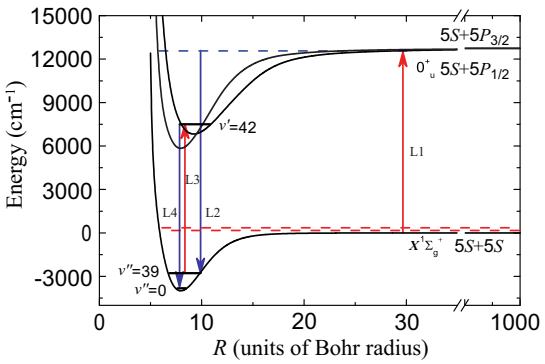

FIG. 1. Schematic diagram of the photoassociation and the subsequent rovibration cooling processes at millikelvin temperature. The initial state related to the ground electronic $X^1\Sigma_g^+$ state and high rovibrational levels (dashed blue line) of the excited electronic 0_u^+ state are coupled by short laser pulse L1. The photoassociated molecules are cooled to the rovibrational ground state via the intermediate states $|v'' = 39\rangle$ and $|v' = 42\rangle$ by laser pulses L2, L3, and L4. The dashed lines just above the $X^1\Sigma_g^+$ state denote the initial continuum state with thermal distribution.

Bruzewicz *et al*. prepared the ground-state RbCs molecules via the photoassociation of ultracold Rb and Cs atoms followed by radiative stabilization [38]. Shimasaki *et al*. prepared the rovibrational ground-state RbCs molecules via two-photon-cascade decay [39]. Mark *et al*. investigated the coherent preparation of the rovibrational ground-state Cs_2 molecules via a multiphoton transfer process [40]. The weakly bound molecules were first prepared by sweeping the magnetic field across the Feshbach resonance from Bose-Einstein condensates of ultracold Cs atoms [41], and two successive two-photon STIRAPs [42] were then used to realize the population transfer from the weakly bound ground state to the rovibrational ground state. Koch *et al*. investigated the formation of ground-state molecules from ultracold cesium atoms in a two-color pump-dump photoassociation with chirped picosecond laser pulses [43]. The vibrational period of the $^{85}Rb_2$ molecular wave packet near the threshold in the excited electronic 0_u^+ $(5S + 5P_{1/2})$ state is about 200 ps. By turning on the picosecond dump laser when the excited electronic wave packet reaches its inner turning point, the transfer efficiency can be considerably enhanced. Many experimental techniques have been developed to observe the photoassociation and rovibrational cooling processes, such as laser-induced fluorescence spectroscopy [33,35], resonantly enhanced multiphoton ionization [44], and rotationally resolved trap-loss spectra [45].

Rovibrational cooling of the photoassociated molecules at millikelvin temperature has been little studied in both experiment and theory. Vibration cooling of the photoassociated molecules lying in the excited electronic state is difficult, because there is no strict selection rule restricting the transition from the excited electronic state to different vibrational levels of the ground electronic state. In the present work, we investigate theoretically the vibration and rotation cooling of the $^{85}Rb_2$ molecule resulting from the photoassociation of ^{85}Rb atoms at millikelvin temperature. We discuss how to convert the photoassociated molecules in the excited state into the stable ultracold molecules in the rovibrational ground state of the ground electronic state.

The paper is organized as follows: The theoretical approach is given in Sec. II. The rovibration cooling of photoassociated molecules at millikelvin temperature is described and discussed in Sec. III. A conclusion is drawn in Sec. IV.

II. THEORETICAL APPROACH

In the photoassociation and the subsequent rovibration cooling processes, two cold colliding ^{85}Rb atoms in the ground electronic $X^1\Sigma_g^+$ $(5S + 5S)$ state are first associated into the Rb_2 molecule in the excited electronic 0_u^+ $(5S + 5P_{1/2})$ state by a picosecond laser pulse L1. The photoassociated molecules on the high rovibrational levels of the 0_u^+ state are then cooled to the rovibrational ground states of the ground electronic $X^1\Sigma_g^+$ $(5S + 5S)$ state by 3-ps laser pulses L2, L3, and L4, as shown in Fig. 1 . The 0_u^+ $(5S + 5P_{1/2})$ and 0_u^+ $(5S + 5P_{3/2})$ states in Hund's case (c) are coupled by the spin-orbit interaction. Within the dipole approximation and rotating-wave approximation, the Hamiltonian describing the photoassociation and laser-cooling processes can be expressed in the diabatic representation as

$$\hat{\mathbf{H}}=\begin{pmatrix} \hat{T}+\hat{V}_{X^1\Sigma_g^+}(R)+\frac{\hat{L}^2}{2\mu R^2} & \hat{\mu}(R)\cdot\hat{E}(t) & 0 \\ \hat{\mu}(R)\cdot\hat{E}(t) & \hat{T}+\hat{V}_{A^1\Sigma_u^+}(R)+\frac{\hat{L}^2}{2\mu R^2}-\hbar\omega_{0i} & \Delta_{\Pi\Sigma} \\ 0 & \Delta_{\Pi\Sigma} & \hat{T}+\hat{V}_{b^3\Pi_u}(R)+\frac{\hat{L}^2}{2\mu R^2}-\Delta_{\Pi\Pi}-\hbar\omega_{0i} \end{pmatrix}, \quad (1)$$

where $\hat{T}$ is the kinetic energy operator and R the interatomic distance. $\hat{L}$ is the angular momentum operator. $\Delta_{\Pi\Pi}$ and $\Delta_{\Pi\Sigma}$ denote the diagonal and off-diagonal spin-orbit couplings, respectively. μ is the reduced mass. ω_{0i} $(i = 1, 2, 3,$ and $4)$ is the laser frequency for laser pulse Li $(i = 1, 2, 3,$ and $4)$. The potential function $\hat{V}_{X^1\Sigma_g^+}(R)$ of the ground electronic $X^1\Sigma_g^+$ state is adopted from Ref. [46]. The potential functions $\hat{V}_{A^1\Sigma_u^+}(R)$ and $\hat{V}_{b^3\Pi_u}(R)$ of the excited $A^1\Sigma_u^+$ and $b^3\Pi_u$ states and the spin-orbit coupling are taken from Ref. [47]. The R-dependent transition dipole moment $\mu(R)$ is obtained from Ref. [48].

The photoassociation and cooling processes can be described by solving the time-dependent Schrödinger equation,

$$i\hbar\frac{\partial}{\partial t}|\Phi(t)\rangle = \hat{\mathbf{H}}(t)|\Phi(t)\rangle, \quad (2)$$

using the mapped Fourier grid Hamiltonian method [49] and the Chebyshev polynomials propagation method [50,51].

The initial-state distribution at thermal equilibrium can be described by the initial density operator

$$\hat{\rho}^T(t_0) = \frac{1}{Z} e^{-\beta \hat{H}_g}, \tag{3}$$

where $\beta = 1/(k_B T)$, with k_B being the Boltzmann constant. T is the temperature and $\hat{H}_g$ is the ground-electronic-state Hamiltonian. $Z = \mathrm{Tr}[e^{-\beta \hat{H}_g}]$ is the partition function. The eigenfunction ψ_{nl} of $\hat{H}_g$ can be used to represent the basis function of the density operator, as in Ref. [52]. We have studied the initial-state distribution at thermal equilibrium and the density operator in detail in Ref. [31]. The weight of $|\psi_{nl}\rangle$ is given by

$$W_{nl} = \frac{1}{4\pi Z}(2l+1)e^{-\beta E_{nl}}. \tag{4}$$

The sum over translational n and rotational l quantum numbers is cut off by the Boltzmann weight [31].

In the photoassociation process, the population in the rovibrational state $|\psi_{v'l_e}\rangle$ of the excited electronic state after propagating the eigenstate $|\psi_{nl}\rangle$ from initial time t_0 to time t is given by

$$P^{nl}_{v'l_e}(t) = |\langle \psi_{v'l_e}|\hat{U}(t,t_0)|\psi_{nl}\rangle|^2, \tag{5}$$

where $\hat{U}(t,t_0)$ is the time-evolution operator. The thermally averaged population of the rovibrational state $|\psi_{v'l_e}\rangle$ of the excited electronic state is expressed as

$$P_{v'l_e} = \sum_{nl} W_{nl} P^{nl}_{v'l_e}. \tag{6}$$

The vibration cooling process is governed by the relevant transition matrix elements. The transition matrix element between the initial eigenstate $|\psi_{nl}\rangle$ and the rovibrational state $|\psi_{v'l_e}\rangle$ of the excited electronic state is calculated by

$$M_{v'l_e,nl} = |\langle \psi_{v'l_e}|\mu(R)|\psi_{nl}\rangle|^2. \tag{7}$$

Due to the thermodynamics effect, the weights W_{nl} of different states $|\psi_{nl}\rangle$ are different. Thus, the Boltzmann weight should be included in the transition matrix element. The weighted transition matrix element is given by

$$M'_{v'l_e,nl} = \frac{e^{-\beta E_{nl}}}{\sum_{n'} e^{-\beta E_{n'l}}} |\langle \psi_{v'l_e}|\mu(R)|\psi_{nl}\rangle|^2. \tag{8}$$

The time-dependent transition matrix element between the rovibrational state $|\psi_{v''l}\rangle$ of the ground electronic state and the excited electronic state $|\psi_{l_e}(t)\rangle$ is given by

$$M_{l_e,v''l}(t) = |\langle \psi_{l_e}(t)|\mu(R)|\psi_{v''l}\rangle|^2. \tag{9}$$

The excited-electronic-state wave packet $|\psi_{l_e}(t)\rangle$ is expressed as

$$|\psi_{l_e}(t)\rangle = \sum_{v'}\sum_{n} \frac{W_{nl}}{\sum_{n'} W_{n'l}} \langle \psi_{v'l_e}|\hat{U}(t,t_0)|\psi_{nl}\rangle|\psi_{v'l_e}\rangle. \tag{10}$$

The rotation cooling process is governed by the angular momentum transition selection rules. The off-diagonal term $\hat{\mu}(R)\cdot\hat{E}(t)$ in Eq. (1) couples different rotational states and its matrix element can be expressed as

$$\langle \mathrm{P}_l|\hat{\mu}(R)\cdot\hat{E}(t)\big|\mathrm{P}_{l_e}\rangle = -\tfrac{1}{2}\mu(R)E_0 f(t) C^{l_e}_l, \tag{11}$$

with

$$C^{l_e}_l = \langle \mathrm{P}_l|\cos\theta\big|\mathrm{P}_{l_e}\rangle. \tag{12}$$

In Eq. (11), $f(t)$ (E_0) denotes the temporal envelope (amplitude) of the laser pulse. l and l_e are the rotational quantum numbers of the ground and excited electronic states, respectively. P_l and P_{l_e} denote the Legendre functions.

The population in the rovibrational state $|\psi_{v''l}\rangle$ of the ground electronic state after propagating the eigenstate $|\psi_{nl}\rangle$ from initial time t_0 to time t is calculated by

$$P^{nl}_{v''l}(t) = |\langle \psi_{v''l}|\hat{U}(t,t_0)|\psi_{nl}\rangle|^2. \tag{13}$$

The thermally averaged population in the rovibrational state of the ground electronic state is given by

$$P_{v''l} = \sum_{nl} W_{nl} P^{nl}_{v''l}. \tag{14}$$

III. RESULTS AND DISCUSSION

The electric field of the laser pulse is expressed as $\widetilde{E}(\omega) = A(\omega)e^{-i\phi(\omega)t}$ in the frequency domain [53]. $\widetilde{E}(\omega)$ is a complex function containing all the information of the laser pulse. $A(\omega) = \exp[-2\ln 2(\omega-\omega_0)^2/\omega_f^2]$ is the spectral amplitude, with ω_f being the FWHM. $\phi(\omega)$ is the spectral phase of the laser pulse. By using the Fourier transform, the electric field of the laser pulse in the time domain of Eq. (1) is given by $E(t) = \frac{1}{2\pi}\int_{-\infty}^{\infty}\widetilde{E}(\omega)e^{-i\omega t}d\omega$. The phase and amplitude of the laser pulse can be modulated by a Fourier transform pulse shaping technique [54]. In order to obtain high cooling efficiency and prepare pure ground-state molecules, the laser pulse parameters used in our calculations are optimized. The spectral phases $\phi(\omega)$ of all laser pulses are taken to be 0. The peak intensities of laser pulses L1, L2, L3, and L4 are chosen as 2.5×10^6, 2.5×10^{10}, 6.0×10^8, and 1.0×10^{10} W/cm^2, respectively. The FWHM of laser pulses L1, L2, L3, and L4 in the frequency domain are taken to be 2.0, 10.0, 1.0, and 10.0 cm^{-1} in order. The evolution time is taken to be 200 ps, with a step size of 0.01 ps, which is much shorter than the lifetimes of the ^{85}Rb($5p^2P_{1/2}$, $5p^2P_{3/2}$) levels and the excited electronic 0^+_u state of the ^{85}Rb$_2$ molecule. Thus the spontaneous emission can be ignored. The range of interatomic distance is taken to be $5-1000$ a_0 (a_0 is the Bohr radius).

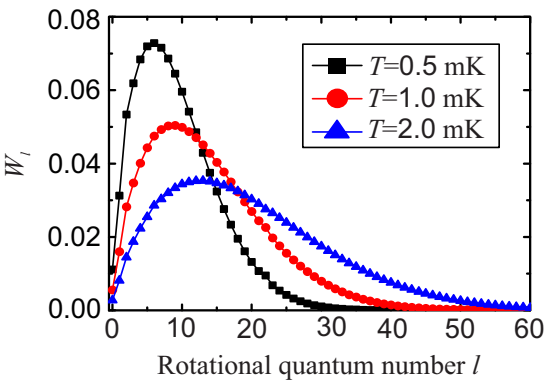

FIG. 2. Weight $W_l = \sum_n W_{nl}$ vs rotational quantum number l at $T = 0.5$, 1, and 2 mK, where W_{nl} is the weight of the $|\psi_{nl}\rangle$ state.

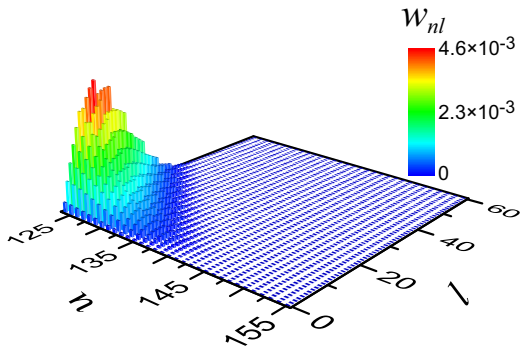

FIG. 3. Weight W_{nl} of $|\psi_{nl}\rangle$ vs translational quantum number n and rotational quantum number l at $T = 2$ mK.

For such a long box, the lowest scattering level with energy $\propto 1/R_{\max}^2$ is in the magnitude order of 10^{-6} K. Therefore the discretization of the continuum states is suitable for the energy of the mK magnitude order.

Figure 2 shows the weight $W_l = \sum_n W_{nl}$ of the initial state versus rotational quantum number l at $T = 0.5$, 1.0, and 2.0 mK. At $T = 0.5$ mK, W_l is mainly distributed in the range of $l = 0 - 30$, and its maximum appears at $l = 6$. When $T = 1.0$ mK, W_l is mostly distributed in the range of $l = 0 - 45$, and its maximum appears at $l = 9$. At $T = 2.0$ mK, W_l is mostly distributed in the range of $l = 0 - 60$, and its maximum is at $l = 13$. As temperature increases, the activated rotational levels increase and a rotational quantum number l corresponding to the maximum of W_l becomes large. Figure 3 shows the weight W_{nl} of $|\psi_{nl}\rangle$ in the ranges of $l = 0$–60 and $n = 124$–155 at $T = 2$ mK. W_{nl} describes the population change with rotational quantum number l and translational quantum number n of the initial scattering state. The distributions of W_{nl} and W_l are determined by the degeneracy factor $(2l + 1)/4\pi$ and the energy-level distribution factor $e^{-\beta E_{nl}}$, respectively. The weighted distributions of the rotational and vibrational states provide a window for us to observe the property of the initial state.

In the photoassociation process, $|l_e = 1\rangle$ is chosen as the target rotational state. The population $P_{v'l_e}$ is mainly determined by the weighted transition matrix elements $M'_{v'l_e,nl}$. The weighted transition matrix elements for $l = 2$, $n = 124$–150, $l_e = 1$, and $v' = 440$–500 are shown in Fig. 4(a). In the design of a laser-cooling scheme, we encounter trouble. The transition matrix element between $|\psi_{v'l_e}\rangle$ and $|\psi_{v''=0,l=0}\rangle$ is very small. Fortunately, the transition matrix elements between $|\psi_{v'l_e}\rangle$ and some deep bound states $|\psi_{v''l}\rangle$ are very large. Thus, we can first transfer the population to the deep bound state and then transfer it to the rovibrational ground state.

The population $P_{v''l}$ of the ground electronic state depends mainly on the transition matrix element $M_{v'l_e,v''l} = |\langle\psi_{v'l_e}|\mu(R)|\psi_{v''l}\rangle|^2$ and the population $P_{v'l_e}$. Figure 4(b) shows the transition matrix element $M_{v'l_e,v''l}$ for $l = 0$, v''=30–45, $l_e = 1$, and $v' = 440$–500. The transition matrix element $M_{v'l_e,v''l}$ reaches its maximum at $v'' = 39$. The weighted transition matrix element $M'_{v'l_e,nl}$ in Fig. 4(a) and the transition matrix element $M_{v'l_e,v''l}$ in Fig. 4(b) are used to determine the central frequencies of laser pulses L1 and L2, respectively. The wave packet of the excited electronic state driven by laser pulse L1 is not a thermodynamic equilibrium state. Therefore, when determining the central frequency of laser pulse L2, we use the transition matrix element $M_{v'l_e,v''l}$ instead of the weighted transition matrix element $M'_{v'l_e,nl}$. In order to get a large rovibrational population $P_{v''l}$ of the ground electronic state, the central frequency ω_{01} of laser pulse L1 is taken to be resonant with the rovibrational state $|\psi_{v'=473,l_e=1}\rangle$ of the excited electronic state, and the central frequency ω_{02} of laser pulse L2 is taken to be resonant with the rovibrational state $|\psi_{v''=39,l_e=0}\rangle$ of the ground electronic state.

After the central frequencies of laser pulses L1 and L2 are determined, the central times of L1 and L2 need to be chosen. The central time of laser pulse L1 is taken to be 25 ps. In order to find an optimal central time of laser pulse L2, we depict the evolution of the excited-electronic-state wave packet in Fig. 5(a) and calculate the time-dependent transition matrix element $M_{l_e,v''l}(t)$ in Fig. 5(b). The wave packet initially moves to short interatomic distance and then moves backward to large interatomic distance. At $t = 105$ ps,

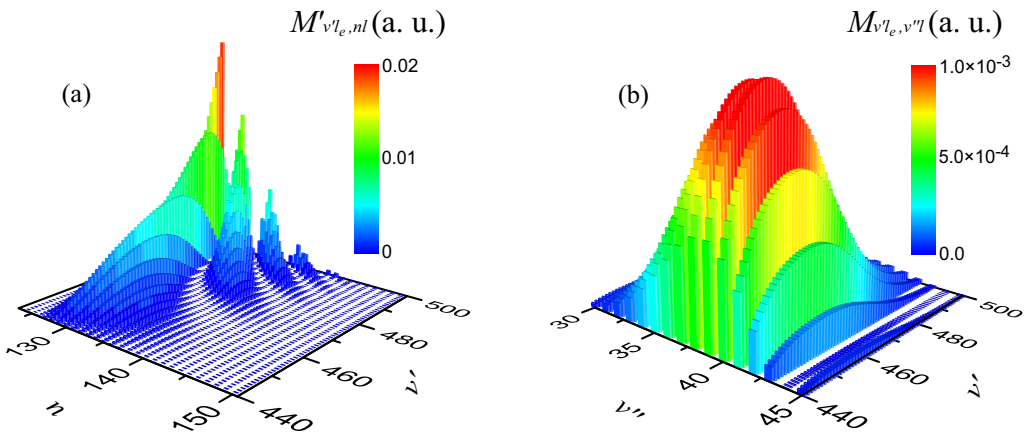

FIG. 4. (a) The weighted transition matrix element $M'_{v'l_e,nl}$ between $|\psi_{nl}\rangle$ and $|\psi_{v'l_e}\rangle$ in the ranges of $l = 2$, $n = 124$–150, $l_e = 1$, and $v' = 440$–500. (b) The transition matrix element $M_{v'l_e,v''l}$ between $|\psi_{v''l}\rangle$ and $|\psi_{v'l_e}\rangle$ in the ranges of $l = 0$, $v'' = 30$–45, $l_e = 1$, and $v' = 440$–500.

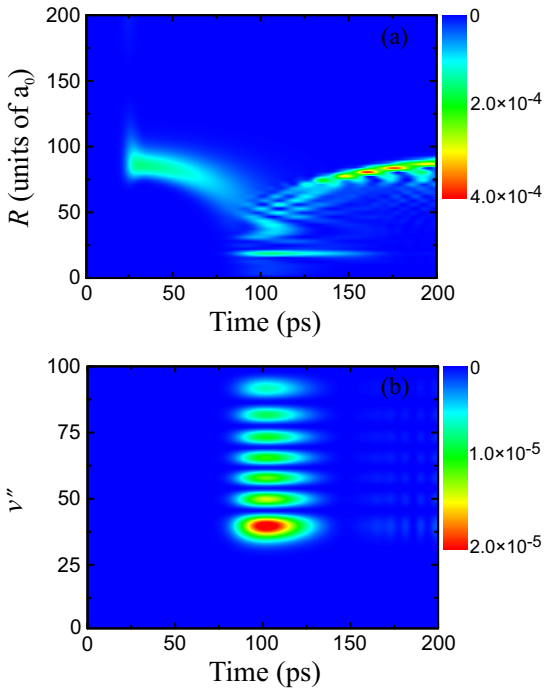

FIG. 5. (a) The excited-electronic-state wave packet $|\psi_{l_e}(t)\rangle$ vs R and time for $l_e = 1$. (b) Time-dependent transition matrix element $M_{l_e,v''l}(t)$ between the excited-electronic-state wave packet for $l_e = 1$ and the rovibrational level of the ground electronic state for $l = 0$, $v'' = 0$–100.

the wave packet enters the short interatomic distance region ($R < 20\ a_0$). The wave function of the deep vibrational state $|v'' = 39\rangle$ is mainly distributed in the interatomic distance range of $R < 7\ a_0$. As shown in Fig. 5(b), the time-dependent transition matrix element $M_{l_e=1,v''=39,l=0}(t)$ reaches its maximum at $t = 105$ ps. Therefore, $t = 105$ ps is an optimal central time of laser pulse L2.

Figure 6 shows the population $P_{v'l_e}$ versus v' and l_e at $t = 90$ ps and $T = 2$ mK. $P_{v'l_e}$ is mostly distributed in the range of $l_e = 0$–8. The maximal contribution to the population of the excited electronic state comes from $l_e = 1$. When $l_e \geqslant 4$,

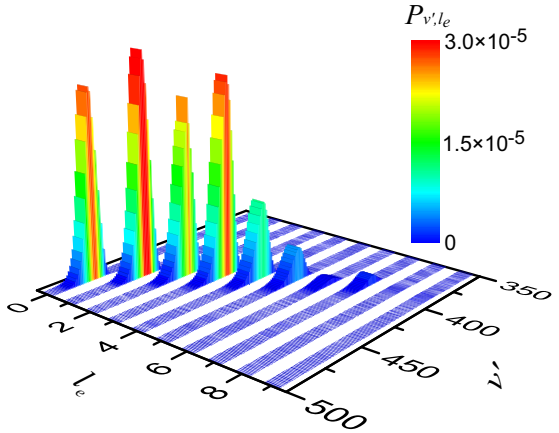

FIG. 6. The thermally averaged population $P_{v'l_e}$ of the rovibrational state $|\psi_{v'l_e}\rangle$ vs v' and l_e at $t = 90$ ps and $T = 2$ mK.

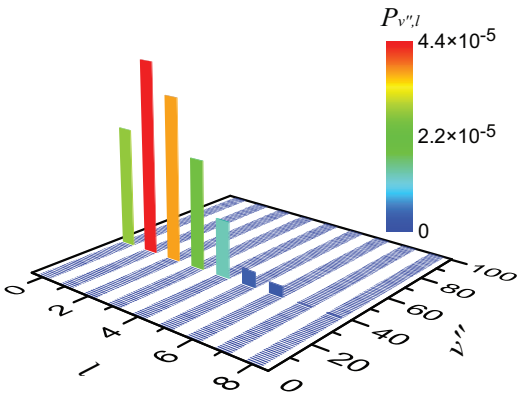

FIG. 7. The thermally averaged population $P_{v''l}$ of the rovibrational state $|\psi_{v''l}\rangle$ for $l = 0$–8 and $v'' = 0$–100 at $T = 2$ mK before laser pulse L3 is turned on.

the population starts to decrease significantly. When $l_e = 9$, the population is close to zero. This is because the weighted transition matrix element is very small when $l_e \geqslant 9$. With the increase of rotational quantum number, the rotational potential barrier of the ground electronic state increases, which restrains the amplitude of the wave function at short interatomic distance. The population $P_{v'l_e}$ is distributed in a wide range of vibrational levels ($v' = 375$–500).

In the laser-cooling process, the photoassociated molecules are first cooled to the deep vibrational level of the ground electronic state by laser pulse L2. Figure 7 shows the rovibrational population $P_{v''l}$ of the ground electronic state for $l = 0$–8 and $v'' = 0$–100 at $T = 2$ mK before laser pulse L3 is turned on. It can be seen that the population $P_{v''l}$ is distributed only on the vibrational level $v'' = 39$. The energy difference between the vibrational level $v'' = 39$ and its neighboring vibrational levels for $l = 0$–8 are all larger than 45 cm^{-1}. However, the FWHM of laser pulse L2 is 10 cm^{-1}. The population $P_l = \sum_{v''=0}^{100} P_{v''l}$ is mostly distributed in the range of $l = 0$–6, and its maximum appears at $l = 1$. The molecules in the deep rovibrational state $|\psi_{v''=39,l=0-6}\rangle$ can be then transferred to the rovibrational ground state $|\psi_{v''=0,l=0}\rangle$.

In order to transfer the population from $|\psi_{v''=39,l=0-6}\rangle$ to $|\psi_{v''=0,l=0}\rangle$, we need to find an appropriate intermediate state in the excited electronic state. Figure 8(a) shows the transition matrix elements $M_{v'l_e=1,v''=39,l=2}$, $M_{v'l_e=1,v''=0,l=0}$ and their product $M_{v'l_e=1,v''=39,l=2} \times M_{v'l_e=1,v''=0,l=0}$, where $M_{v'l_e=1,v''=39,l=2}$ denotes the transition matrix element between the deep rovibrational state $|\psi_{v''=39,l=2}\rangle$ of the ground electronic state and the rovibrational state $|\psi_{v',l_e=1}\rangle$ of the excited electronic state. $M_{v'l_e=1,v''=0,l=0}$ denotes the transition matrix element between the rovibrational ground state $|\psi_{v''=0,l=0}\rangle$ of the ground electronic state and the rovibrational state $|\psi_{v',l_e=1}\rangle$ of the excited electronic state. As can be seen from Fig. 8(a), when $v' = 42$, the product $M_{v'l_e=1,v''=39,l=2} \times M_{v'l_e=1,v''=0,l=0}$ reaches its maximum value. Therefore, we choose $|\psi_{v'=42,l_e=1}\rangle$ as the intermediate state. Thus, the central frequencies ω_{03} and ω_{04} of laser pulses L3 and L4 are taken to be 9356.86 and 11 375.62 cm^{-1}, respectively.

The $^{85}Rb_2$ molecule in the deep rovibrational states $|\psi_{v''=39,l=0-6}\rangle$ is then cooled to the rovibrational ground state

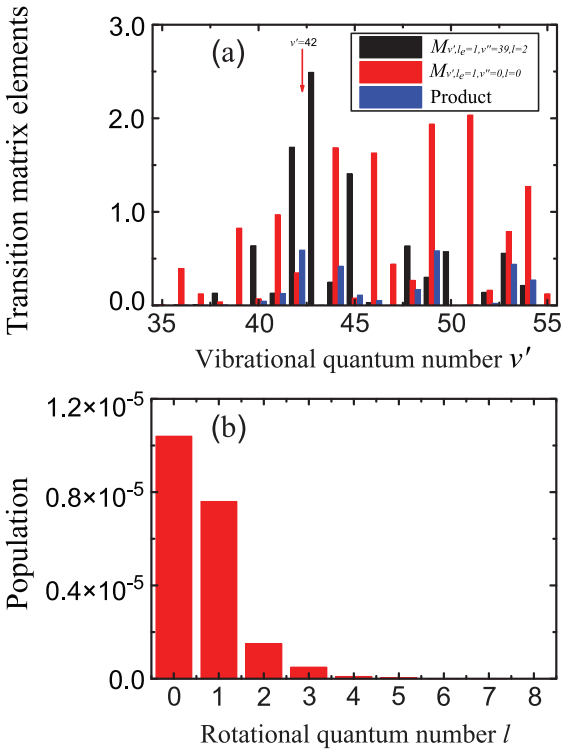

FIG. 8. (a) The transition matrix elements $M_{v'l_e=1,v''=39,l=2}$, $M_{v'l_e=1,v''=0,l=0}$, and the product $M_{v'l_e=1,v''=39,l=2} \times M_{v'l_e=1,v''=0,l=0}$. (b) The thermally averaged population $P_{v''=0,l}$ vs rotational quantum numbers l of the ground state $|\psi_{v''=0,l}\rangle$.

$|\psi_{v''=0,l=0}\rangle$ by laser pulses L3 and L4. The population of the ground electronic state transferred from the intermediate state $|\psi_{v'=42,l_e=1}\rangle$ is fully distributed only in the vibrational ground state $|v''=0\rangle$, indicating that the vibration cooling efficiency is very high. As shown in Fig. 8(b), the thermally averaged population $P_{v''=0,l=0}$ of the rovibrational ground state $|\psi_{v''=0,l=0}\rangle$ is 1.04×10^{-5}. The thermally averaged population being of the order of 10^{-5} is in a reasonable range. In the experiments of conversion of ^{41}K and ^{87}Rb atoms into ultracold ^{41}K^{87}Rb molecules by laser cooling, the conversion probability was of the order of 10^{-5}–10^{-4} [37]. In the experiments of preparing the ultracold LiCs molecules in the ground state via photoassociation, the conversion probability was of the order of 10^{-5} [55]. In the experiment of the vibration cooling of Cs_2 molecules in the ground electronic state, the transferred population was of the order of 10^{-4} [56,57]. We can see from Fig. 8(b) that 51.59% of the population in the vibrational ground state is concentrated in the rotational ground state $|l=0\rangle$. The rest of the population in the vibrational ground state is distributed in the rotational states $|l=1-3\rangle$.

IV. CONCLUSION

In this paper, we have investigated theoretically the vibration and rotation cooling of the $^{85}Rb_2$ molecule resulting from the photoassociation of ^{85}Rb atoms at millikelvin temperature. At temperature $T=2.0$ mK, the weight W_{nl} of $|\psi_{nl}\rangle$ is mainly distributed in the ranges of $l=0$–60 and $n=124$–155. The population $P_{v'l_e}$ of the associated $^{85}Rb_2$ molecule in the excited electronic state is distributed in hundreds of rovibrational states. Since the transition matrix elements between $|\psi_{v'l_e}\rangle$ and $|\psi_{v''=0,l=0}\rangle$ are very small, we first transfer the population to the deep vibrational state $|\psi_{v''=39}\rangle$ and then transfer it to the rovibrational ground state $|\psi_{v''=0,l=0}\rangle$ via the intermediate state $|\psi_{v'=42,l_e=1}\rangle$. After the cooling process is over, the population transferred from the intermediate state $|\psi_{v'=42,l_e=1}\rangle$ is fully distributed in vibrational ground state $|v''=0\rangle$, and 51.59% of population in the vibrational ground state $|v''=0\rangle$ is concentrated in the rotational ground state $|l=0\rangle$. The rest of the population in the $|v''=0\rangle$ state is distributed in the low rotational states $|l=1$–$3\rangle$.

ACKNOWLEDGMENTS

This work is supported by the National Key R&D Program of China under Grant No. 2018YFA0306503 and by the National Natural Science Foundation of China under Grants No. 11274056 and No. 11774043.

[1] A. Micheli, G. K. Brennen, and P. Zoller, Nat. Phys. **2**, 341 (2006).
[2] D. DeMille, Phys. Rev. Lett. **88**, 067901 (2002).
[3] P. Rabl, D. DeMille, J. M. Doyle, M. D. Lukin, R. J. Schoelkopf, and P. Zoller, Phys. Rev. Lett. **97**, 033003 (2006).
[4] E. R. Hudson, H. J. Lewandowski, B. C. Sawyer, and J. Ye, Phys. Rev. Lett. **96**, 143004 (2006).
[5] T. Zelevinsky, S. Kotochigova, and J. Ye, Phys. Rev. Lett. **100**, 043201 (2008).
[6] R. V. Krems, Int. Rev. Phys. Chem. **24**, 99 (2005).
[7] M. E. Wagshul, K. Helmerson, P. D. Lett, S. L. Rolston, W. D. Phillips, R. Heather, and P. S. Julienne, Phys. Rev. Lett. **70**, 2074 (1993).
[8] J. D. Miller, R. A. Cline, and D. J. Heinzen, Phys. Rev. Lett. **71**, 2204 (1993).
[9] B. J. Lester, N. Luick, A. M. Kaufman, C. M. Reynolds, and C. A. Regal, Phys. Rev. Lett. **115**, 073003 (2015).
[10] L. R. Liu, J. D. Hood, Y. Yu, J. T. Zhang, N. R. Hutzler, T. Rosenband, and K.-K. Ni, Science **360**, 900 (2018).
[11] Z. H. Li, T. Gong, Z. H. Ji, Y. T. Zhao, L. T. Xiao, and S. T. Jia, Phys. Chem. Chem. Phys. **20**, 4893 (2018).
[12] J. L. Carini, S. Kallush, R. Kosloff, and P. L. Gould, J. Phys. Chem. A **120**, 3032 (2016).
[13] E. Pachomow, V. P. Dahlke, E. Tiemann, F. Riehle, and U. Sterr, Phys. Rev. A **95**, 043422 (2017).
[14] J. H. Han, J. H. Kang, M. Lee, and Y. Shin, Phys. Rev. A **97**, 013401 (2018).
[15] E. F. de Lima, Phys. Rev. A **95**, 013411 (2017).
[16] J. Ulmanis, J. Deiglmayr, M. Repp, R. Wester, and M. Weidemüller, Chem. Rev. **112**, 4890 (2012).

[17] T. M. Rvachov, H. Son, J. J. Park, P. M. Notz, T. T. Wang, M. W. Zwierlein, W. Ketterle, and A. O. Jamison, Phys. Chem. Chem. Phys. **20**, 4746 (2018).
[18] Y. C. Han, J. W. Hu, and B. B. Wang, Phys. Rev. A **98**, 043420 (2018).
[19] M. Wang, M. D. Chen, X. J. Hu, J. L. Li, and S. L. Cong, Laser Phys. **26**, 055005 (2016).
[20] W. Zhang, Y. Huang, T. Xie, G. R. Wang, and S. L. Cong, Phys. Rev. A **82**, 063411 (2010).
[21] E. Luc-Koenig, R. Kosloff, F. Masnou-Seeuws, and M. Vatasescu, Phys. Rev. A **70**, 033414 (2004).
[22] J. L. Carini, S. Kallush, R. Kosloff, and P. L. Gould, Phys. Rev. Lett. **115**, 173003 (2015).
[23] W. Salzmann, T. Mullins, J. Eng, M. Albert, R. Wester, M. Weidemüller, A. Merli, S. M. Weber, F. Sauer, M. Plewicki, F. Weise, L. Wöste, and A. Lindinger, Phys. Rev. Lett. **100**, 233003 (2008).
[24] D. B. Blasing, I. C. Stevenson, J. Pérez-Rios, D. S. Elliott, and Y. P. Chen, Phys. Rev. A **94**, 062504 (2016).
[25] K. M. Jones, E. Tiesinga, P. D. Lett, and P. S. Julienne, Rev. Mod. Phys. **78**, 483 (2006).
[26] H. M. J. M. Boesten, C. C. Tsai, B. J. Verhaar, and D. J. Heinzen, Phys. Rev. Lett. **77**, 5194 (1996).
[27] M. A. Bellos, R. Carollo, D. Rahmlow, J. Banerjee, E. E. Eyler, P. L. Gould, and W. C. Stwalley, Phys. Rev. A **86**, 033407 (2012).
[28] K. Sakimoto, Phys. Rev. A **94**, 042701 (2016).
[29] W. Skomorowski, Y. Shagam, E. Narevicius, and C. P. Koch, J. Phys. Chem. A **120**, 3309 (2016).
[30] R. González-Férez and C. P. Koch, Phys. Rev. A **86**, 063420 (2012).
[31] M. Wang, J. L. Li, X. J. Hu, M. D. Chen, and S. L. Cong, Phys. Rev. A **96**, 043417 (2017).
[32] S. Amaran, R. Kosloff, M. Tomza, W. Skomorowski, F. Pawowski, R. Moszynski, L. Rybak, L. Levin, Z. Amitay, J. M. Berglund, D. M. Reich, and C. P. Koch, J. Chem. Phys. **139**, 164124 (2013).
[33] J. R. Gardner, R. A. Cline, J. D. Miller, D. J. Heinzen, H. M. J. M. Boesten, and B. J. Verhaar, Phys. Rev. Lett. **74**, 3764 (1995).
[34] G. Zinner, T. Binnewies, F. Riehle, and E. Tiemann, Phys. Rev. Lett. **85**, 2292 (2000).
[35] L. Rybak, S. Amaran, L. Levin, M. Tomza, R. Moszynski, R. Kosloff, C. P. Koch, and Z. Amitay, Phys. Rev. Lett. **107**, 273001 (2011).
[36] L. Levin, W. Skomorowski, L. Rybak, R. Kosloff, C. P. Koch, and Z. Amitay, Phys. Rev. Lett. **114**, 233003 (2015).
[37] K. Aikawa, D. Akamatsu, M. Hayashi, K. Oasa, J. Kobayashi, P. Naidon, T. Kishimoto, M. Ueda, and S. Inouye, Phys. Rev. Lett. **105**, 203001 (2010).
[38] C. D. Bruzewicz, M. Gustavsson, T. Shimasaki, and D. DeMille, New J. Phys. **16**, 023018 (2014).
[39] T. Shimasaki, M. Bellos, C. D. Bruzewicz, Z. Lasner, and D. DeMille, Phys. Rev. A **91**, 021401(R) (2015).
[40] M. J. Mark, J. G. Danzl, E. Haller, M. Gustavsson, N. Bouloufa, O. Dulieu, H. Salami, T. Bergeman, H. Ritsch, R. Hart, and H.-C. Nägerl, Appl. Phys. B **95**, 219 (2009).
[41] J. Herbig, T. Kraemer, M. Mark, T. Weber, C. Chin, H. C. Nägerl, and R. Grimm, Science **301**, 1510 (2003).
[42] J. G. Danzl, E. Haller, M. Gustavsson, M. J. Mark, R. Hart, N. Bouloufa, O. Dulieu, H. Ritsch, and H.-C. Nägerl, Science **321**, 1062 (2008).
[43] C. P. Koch, E. Luc-Koenig, and F. Masnou-Seeuws, Phys. Rev. A **73**, 033408 (2006).
[44] M. A. Bellos, D. Rahmlow, R. Carollo, J. Banerjee, O. Dulieu, A. Gerdes, E. E. Eyler, P. L. Gould, and W. C. Stwalley, Phys. Chem. Chem. Phys. **13**, 18880 (2011).
[45] Y. Huang, J. Qi, H. K. Pechkis, D. Wang, E. E. Eyler, P. L. Gould, and W. C. Stwalley, J. Phys. B: At. Mol. Opt. Phys. **39**, S857 (2006).
[46] J. Y. Seto, R. J. Le Roy, J. Vergès, and C. Amiot, J. Chem. Phys. **113**, 3067 (2000).
[47] T. Bergeman, J. Qi, D. Wang, Y. Huang, H. K. Pechkis, E. E. Eyler, P. L. Gould, W. C. Stwalley, R. A. Cline, J. D. Miller, and D. J. Heinzen, J. Phys. B: At. Mol. Opt. Phys. **39**, S813 (2006).
[48] R. Beuc, M. Movre, V. Horvatic, C. Vadla, O. Dulieu, and M. Aymar, Phys. Rev. A **75**, 032512 (2007).
[49] K. Willner, O. Dulieu, and F. Masnou-Seeuws, J. Chem. Phys. **120**, 548 (2004).
[50] H. Tal-Ezer and R. Kosloff, J. Chem. Phys. **81**, 3967 (1984).
[51] R. Kosloff, J. Phys. Chem. **92**, 2087 (1988).
[52] C. P. Koch, R. Kosloff, E. Luc-Koenig, F. Masnou-Seeuws, and A. Crubellier, J. Phys. B: At. Mol. Opt. Phys. **39**, S1017 (2006).
[53] A. Monmayrant, S. Weber, and B. Chatel, J. Phys. B: At. Mol. Opt. Phys. **43**, 103001 (2010).
[54] A. M. Weiner, J. P. Heritage, and E. M. Kirschner, J. Opt. Soc. Am. B **5**, 1563 (1988).
[55] J. Deiglmayr, A. Grochola, M. Repp, K. Mörtlbauer, C. Glück, J. Lange, O. Dulieu, R. Wester, and M. Weidemüller, Phys. Rev. Lett. **101**, 133004 (2008).
[56] M. Viteau, A. Chotia, M. Allegrini, N. Bouloufa, O. Dulieu, D. Comparat, and P. Pillet, Science **321**, 232 (2008).
[57] A. Fioretti, D. Comparat, A. Crubellier, O. Dulieu, F. Masnou-Seeuws, and P. Pillet, Phys. Rev. Lett. **80**, 4402 (1998).